Awareness and Filling-in of the Human Blind Spot: Linking Psychophysics with Retinal Topography

Richard V. Abadi,[1,3] *Glen Jeffery,*[2] *and Jonathan S. Murphy*[3]

Purpose. To link psychophysical thresholds for blind spot awareness and filling-in with early neural components that underpin these perceptions.

Methods. Blind spot dimensions were quantified, after which an intrinsic stimulus (i.e., a rectangular bar of varying length centered within the blind spot) was used to determine blind spot awareness and filling-in for five subjects. Histologic examination of six human retinas at 20-μm intervals from the temporal and nasal neural rims of the optic nerve head out to 1040 μm allowed the quantification of outer nuclear layer thickness, a direct correlate of photoreceptor density.

Results. Blind spot awareness was reported for bar extensions beyond 0.4° to 0.8° from the edge of the blind spot. Partial and total blind spot filling-in were reported between 1.1° and 1.3° and beyond 1.5°, respectively. Histologic measures of ONL thickness were correlated with previously published data of photoreceptor spatial density to determine the percentage of photoreceptor density required to trigger a 75% probability response. Blind spot awareness was achieved by stimulating 43% to 70% of the maximum photoreceptor density. Partial and total filling-in of the blind spot required between 78% and 83% and more than 85% photoreceptor spatial densities, respectively.

Conclusions. A novel intrinsic stimulus has been used to concurrently investigate blind spot awareness and blind spot filling-in. Retinal neural correlates of each visual experience have been quantified. Future computational models will have to integrate bottom-up constraints with long-range cortical receptive field activity and higher order cognitive factors. (*Invest Ophthalmol Vis Sci.* 2011;52:541–548) DOI:10.1167/iovs.10-5910

The optic nerve is a photoreceptor-free zone. Its intraocular portion, the optic disc, is positioned approximately 15° temporal to the fovea and has a vertically oval shape approximately corresponding to a visual angle of 7.5° × 5.5°.[1–3] Surprisingly, the consequence of this significant receptor gap does not present a conscious visual problem, even though its extent would comfortably engulf an area equivalent to more than 70 full moons.[4] This is because during binocular viewing, the monocular visual fields overlap such that each field overlays the contralateral blind spot, whereas under monocular conditions, the missing part of the visual field is neurally "filled-in."[5–9]

Over the years many psychophysical studies have characterized the spatial and temporal characteristics of filling-in (completion) by using a variety of achromatic and chromatic stimuli.[7,10–14] These stimuli have been positioned either exclusively outside (i.e., an extrinsic stimulus presentation (Figs. 1a, 1b),[10,14] or both outside and (to some extent) inside the region corresponding to the blind spot (i.e., extrinsic and intrinsic stimuli presentations (Fig. 1c).[11–13] For exclusively extrinsic stimuli, the strength and speed of the completion of the blind spot are strongly dependent on the contrast, texture, and spatial dimensions of the stimulus, but in stimuli with both extrinsic and intrinsic components (such as narrow collinear bars that invade the blind spot), filling-in is proportional to the gap size.[11,13]

To date, the vast majority of filling-in studies have used extrinsic stimuli, and underlying mechanisms have been interpreted in terms of lateral interpolations of neural signals originating from stimuli falling on retinal areas nearest to the rim of the blind spot.[8,9,15–17] These models generally reflect the experimental methodologies, as when collinear bars are placed on either side of the blind spot and the gap between the two leading edges of the bars is narrowed until completion is first reported. Although gap size is an important measure, extrinsic stimuli presentation does not allow a separate judgment of blind spot awareness and so undermines the generality of any resultant model.

In our present study, both awareness and filling in of the blind spot will be separately examined using a horizontal, rectangular bar positioned within the region of visual space corresponding to the blind spot (Figs. 1d, 2). By recording the effects of extending the stimulus beyond the boundaries of the blind spot (Figs. 2c–e), we will first determine the bar length beyond the blind spot border required to generate an awareness of the blind spot (Fig. 2c, two blobs) and thereafter will determine the spatial location at which partial completion (Fig. 2d, bar with a ghosted center) and total completion (Fig. 2e, continuous homogeneous bar) occur. We believe that this technique will allow us to investigate concurrently both blind spot awareness and filling-in and to avoid the strong suprathreshold confounds that occur when using predominantly extrinsic stimuli. Furthermore, our novel technique will allow us to correlate awareness and filling-in with a previously uninvestigated neural correlate—the spatial density of the photoreceptors in the area of the visual field corresponding to the stimulus location.

Directly linking human psychophysical data with human retinal morphology is not a straightforward task. To date, only one study has described the photoreceptor topography in the area around the optic nerve head in humans.[18] Although this

From the [1]Faculty of Life Sciences, University of Manchester, Manchester, United Kingdom; [2]Institute of Ophthalmology, UCL (University College London), London, United Kingdom; and [3]Department of Psychology, NUI (National University of Ireland) Maynooth, Maynooth, Ireland.

Supported by a Science Foundation Ireland Walton Fellowship (RVA) and the Irish Research Council for Science, Engineering and Technology (JSM).

Submitted for publication May 19, 2010; revised July 30, 2010; accepted August 10, 2010.

Disclosure: **R.V. Abadi**, None; **G. Jeffery**, None; **J.S. Murphy**, None

Corresponding author: Richard V. Abadi, University of Manchester, Faculty of Life Sciences, Vision Science Lab, Moffat Building, Sackville Street, Manchester M60 1QD, United Kingdom; r.abadi@manchester.ac.uk.

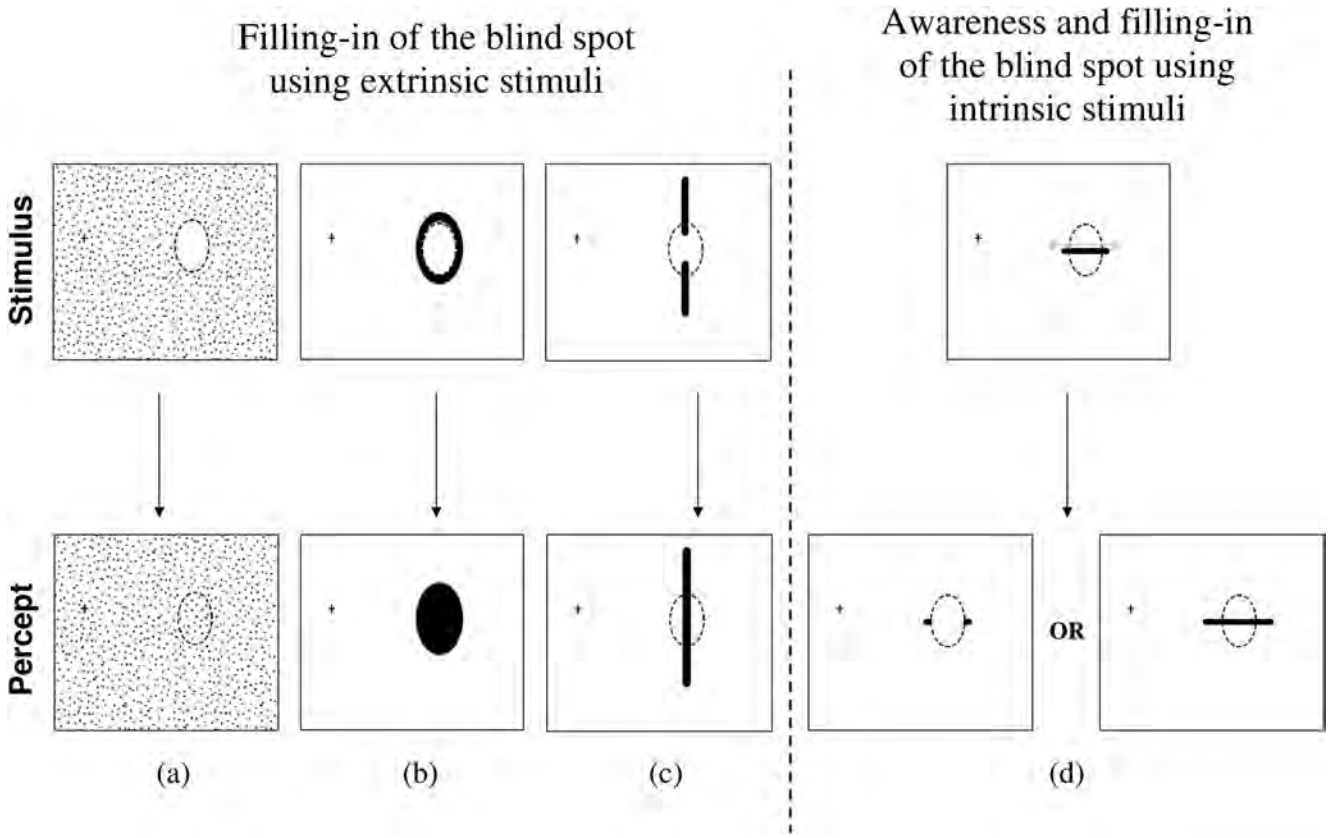

FIGURE 1. Schematic illustration depicting a selection of methodologies that have been used to investigate the nature of filling-in of the blind spot. Stimuli can be presented either exclusively outside (**a**, **b**) or both outside and a little way inside the region corresponding to the blind spot (**c**). Typically, subjects are requested to report when the physical stimulus or stimuli is or are perceived to be continuous. In such cases, filling-in is driven by extrapolation or interpolation of the visible stimuli to the blind spot. Stimuli that lie predominantly inside the blind spot and extend a little way beyond the blind spot boundaries may also give rise to 1 of 2 possibilities (**d**): blind spot awareness (*left*) or filling-in of the blind spot (*right*).

classic histologic study was principally directed at retinal areas away from the optic nerve head, it did provide data on one subject for a small section of the temporal retina adjacent to the rim of the optic nerve head. Counting individual photoreceptors located around the optic nerve head is challenging, especially for large numbers of eyes. Significantly, each photoreceptor has a nucleus in the outer nuclear layer (ONL), the thickness of which reflects the photoreceptor density.[1–3,18,19] By histologically examining human retinal sections close to the rim of the optic nerve head, we sought to correlate ONL thickness and, hence, photoreceptor density, with the psychophysical likelihoods of blind spot awareness and the perception of filling-in.

Materials and Methods

Psychophysics

Mapping the Blind Spot Dimensions. Five subjects (age range, 22–62 years) naive to the purpose of the study took part in all experiments. All tasks were carried out with chin and forehead support and under right monocular viewing conditions at 57 cm from the monitor, which subtended a screen area of 33.5° × 27°. Subjects were requested to fixate a central cross (1° × 1°) at all times. The position and spatial extent of the blind spot was mapped onto a uniform dark gray display (Dell E173FP monitor: 1280 × 1024 pixels; refresh rate 60 Hz; 0.10 cd/m^2). Circular 1.0° stimuli (54% contrast, 200-ms duration) were randomly presented 504 times within a 14° × 12° matrix in and around the area of the visual field corresponding to the blind spot. A conventional "probability map of target detection" demarcated the coarse spatial position, size, and shape of the blind spot (Fig. 3a). A more detailed spatial map of a specific section across the blind spot was subsequently investigated using a smaller horizontal rectangular matrix (15 × 7 half-degree; Fig. 3b). This second map allowed a far more accurate exploration of the blind spot's horizontal boundary within this section, through which our test stimuli would be presented. To further improve spatial resolution, a smaller, circular 0.5 deg° and an increased number of random presentations (n = 525) were adopted across the cell matrix.

Quantifying Awareness and Filling-in of the Human Blind Spot. A rectangular bar (contrast, 54%) 0.5° in width was positioned within and along the minor axis of the blind spot and placed symmetrically within the inner and outer boundaries of the blind spot (Figs. 2, 3c). Both leading edges of the bar had convex curvatures approximating the left and right curvatures of the blind spot borders. Before each trial began, the exact symmetrical alignment of the bar within the blind spot was accomplished by arranging that all subjects reported the presence of two equivalently sized blobs (either side of the blind spot) whenever the bar began to physically extend beyond the previously quantified blind spot boundary (Fig. 2c). Awareness of either a single blob or of two asymmetrically sized blobs indicated that the intrinsically sighted bar had not been positioned symmetrically with respect to the borders of the blind spot (Fig. 3c).

Twenty bar lengths (varying by increments of 6 min arc) were randomly presented, and subjects were asked to respond to 1 of 2 alternative perceptions in experiment 1: "2 blobs" or "a continuous bar" regardless of the bar's perceived uniformity (Fig. 1d). In experi-

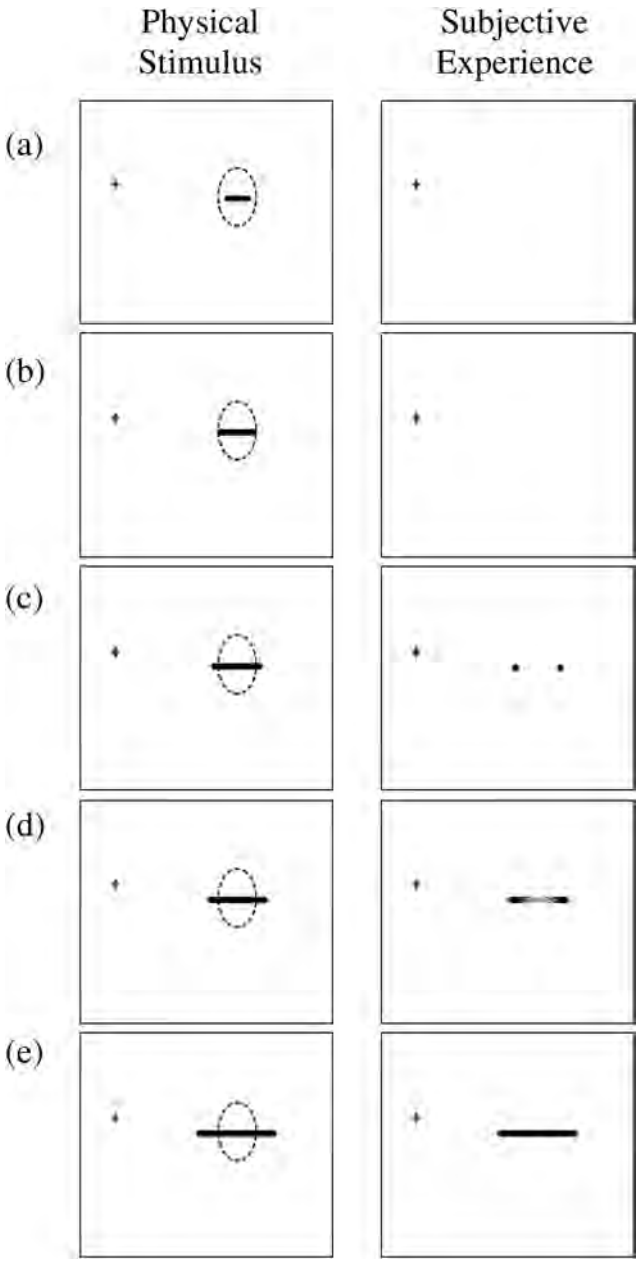

FIGURE 2. Schematic illustration depicting the experimental arrangement during right monocular viewing. The *cross* and *dotted oval* correspond to the fixation and blind spot positions, respectively, within the visual field. The physical stimulus (*left*) and the corresponding subjective experience (*right*) are shown. No component of the bar stimulus is detected when the bar is (**a**) within or (**b**) equivalent to the blind spot width. However, when the bar falls outside the blind spot (**c**–**e**) and excites the functional retina, three levels of subjective experience can be recorded: (**c**) two separate blobs, (**d**) a continuous bar with a ghosted center, and (**e**) a continuous homogeneous bar.

ment 2, subjects were asked to respond to 1 of 3 alternative perceptions: "2 blobs" (Fig. 2c), "a bar with a ghosted center" (Fig. 2d), and "a bar with a uniform appearance" (Fig. 2e). Seventy-five percent threshold values were computed. For experiments 1 and 2, the stimulus presentation time was set at 200 ms.

Histology of the Human Retina Adjacent to the Optic Nerve Head

Six human eyes from separate donors (mean age, 66.2 ± 9.8; age range, 48–77 years; all male) were obtained from the donor eye banks at Moorfields Eye Hospital (London, UK) and the Bristol Eye Hospital (Bristol, UK) within approximately 48 hours of death and were stored in 10% formaldehyde in phosphate-buffered saline (pH 7.2).

An area of retina and underlying choroid and sclera (approximately 1 cm^2 and centered on the optic nerve head) was dissected and cryoprotected in 30% sucrose in 0.1 M phosphate-buffered 4% formaldehyde for 24 hours at room temperature. It was then embedded in gel-album/2.5% glutaraldehyde to provide support during sectioning. Frozen sections were cut at thicknesses of 50 μm. Every section was stored in 4% paraformaldehyde in 0.1 M phosphate buffer at 4°C in individually numbered wells. Wet sections were mounted on slides using phosphate-buffered saline and a standard coverglass. All sections were examined in a fully hydrated condition.

The thickness of the ONL was measured using Nomarski differential contrast microscopy with a microscope (BHZ; Olympus, Tokyo, Japan). Final magnification was 200×. ONL thicknesses were measured at 20-μm intervals up to 740 μm in all six eyes. Tissue quality allowed four eyes (mean age, 71.0 ± 4.5 years; age range, 67–77 years) to be examined (at 20-μm intervals) beyond 740 μm, by a further 300 μm, up to 1040 μm from both the temporal and the nasal rims of the optic nerve. All ONL thickness measurements always began with retinal tissue from the temporal border of the intraocular portion of the optic nerve head; when completed, the nasal border retinal tissue was thereafter examined.

No donor eyes had a history of ocular abnormality, and the optic nerves and retinas appeared normal by gross examination during dissection. Full local ethical committee consent was obtained both for the psychophysical and the anatomic research studies. The experimental and clinical protocol adhered to the tenets of the Declaration of Helsinki.

RESULTS

Standardizing the Blind Spot Boundary

Starting conditions for the locations of the intrinsically placed bars were dependent on the position and spatial extent of each individual's blind spot and based on the horizontal boundary maps (Fig. 3c). To circumvent the variability in blind spot dimensions among our subject group, any reference to bar length will be with respect to the blind spot boundary. That is, the blind spot boundary represents our zero position.

Experiment 1: Detection of Blobs or a Bar

Figure 4 illustrates the averaged response probability functions for detecting either two separate blobs (●) or a bar (■). The vertical line orthogonal to the abscissa at 0 demarcates the edge of the blind spot, with the gray area to its left corresponding to a 0.5° incursion into the blind spot. The first five data points depict a near zero detection rate for perception of the two blobs and the bar because stimuli were still located within the boundaries of the blind spot. As the bar length increased beyond the edge of the blind spot, the probability of detecting two blobs (i.e., blind spot awareness) also increased. This detection rate reached maximum levels when the bar protruded between 0.4° and 0.8° from the edge of the blind spot. Thereafter, the probability of detecting the bar steadily increased. The 75% bar detection threshold was reached when the bar had protruded 1.25° beyond the edge of the blind spot.

Experiment 2: Detection of Blobs, a Bar with a Ghosted Centre, and a Uniform Bar

The response probabilities of detecting two blobs (●), a bar with a ghosted center (■), and a bar with a uniform appearance (■) are shown in Figure 5. Typically, ghosted and uniform bars became noticeable when the bar was extended beyond 1.0° (range, 1.0°-1.3°) and 1.5°, respectively, from

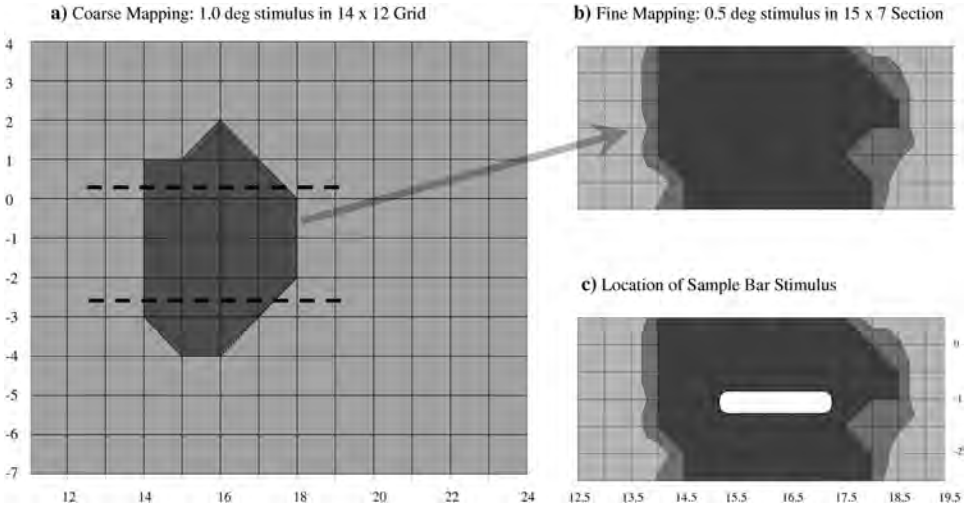

Figure 3. Illustration of the shape and size of the blind spot of the right eye for subject 3. (**a**) Coarse evaluation of the blind spot. 1° circular stimuli were randomly presented a total of 504 times covering a 14° × 12° matrix. The blind spot is demarcated by the *dark gray* area (horizontally 14° to 18° and vertically +2° to −4° deg). Axes indicate the location of the blind spot relative to the fixation cross, which is located nasal to the blind spot. *Horizontal plotted lines*: specific area subsequently investigated in greater detail (**b**, **c**). (**b**) Fine evaluation of the blind spot. 0.5° circular stimuli were randomly presented a total of 525 times covering a 15° × 7° matrix. The blind spot (100% unseen) is demarcated by the *dark gray* area with the *lighter gray* boundary equivalent to 60% unseen. (**c**) To investigate awareness and filling-in of the blind spot, a bar is positioned centrally along the minor axis in a meridian corresponding to 1° below the fixation level. Note that the location of this meridian will vary across the subject group because it is dependent on the overall shape and size of each individual's blind spot.

the edges of the blind spot. By extending the categories of choice, we were able to emphasize the importance of top-down processing, reflected in the higher thresholds found for filling-in of the blind spot in experiment 2 (1.25° vs. 1.5°; compare Figs. 4 and 5).

Histology of the ONL Thickness

Figure 6 shows a horizontal section through the human retina near the nasal border of the optic nerve head.

Figure 7 illustrates how the thickness of the ONL varies as a function of retinal eccentricity for retinal locations up to 740 μm from both temporal and nasal edges of the optic nerve head for the six donor eyes (■). The first samples, taken 20 μm from the optic nerve rim, show identical mean nasal and temporal ONL thicknesses of 20 ± 4.7 μm (n = 6). These values gradually increased to mean nasal and temporal ONL thickness levels of 60.8 ± 7.5 μm and 59.2 ± 9.1 μm, respectively, at the 740-μm location. Corresponding functions for the four eyes examined up to eccentricities of 1040 μm are also plotted (□). No statistically significant asymmetries were found between the temporal and nasal functions for the two data sets (Pearson's correlation, r = 0.99: two-tailed). Best-fit polynomial functions indicated that maximum ONL thickness levels for the nasal retinas were reached by 66.3 μm (n = 6) and 59.0 μm (n = 4) and by 66.0 μm (n = 6) and 66.3 μm (n = 4) for temporal retinas.

Discussion

This study set out to investigate the nature of subjective awareness and filling-in of the blind spot. More specifically, we sought to investigate the retinal neural components that may underpin such perceptual behaviors. Using a bar stimulus positioned within the blind spot, subjects were tasked to report when the previously unseen bar was first perceived, as two blobs or as a bar, when the length of the bar was increased beyond the blind spot boundaries and onto functional retinal tissue. In addition, we determined, from human eyes, the ONL

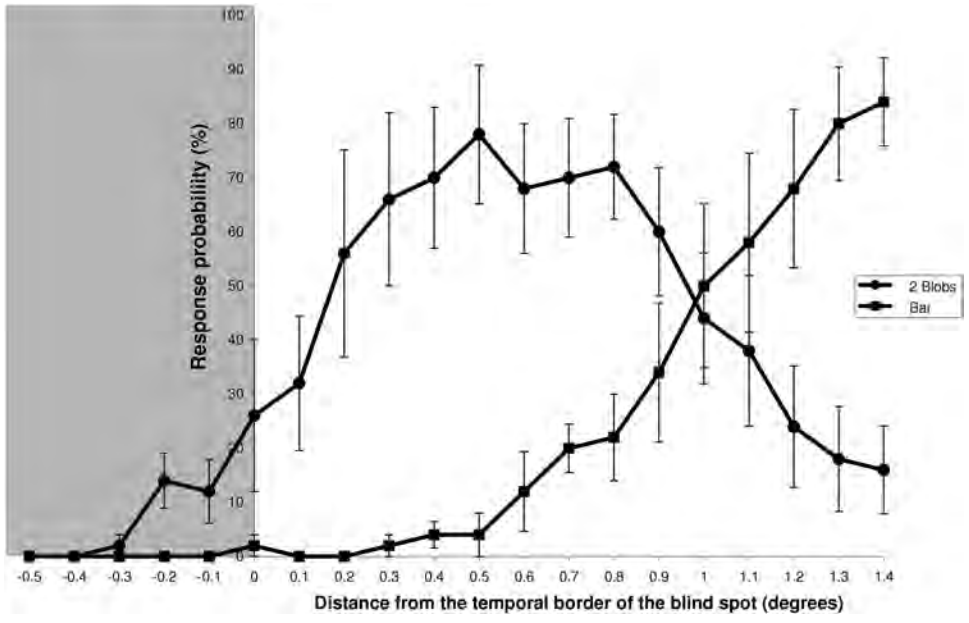

Figure 4. The relationship between the length of the bar extending beyond the blind spot boundary and the corresponding response probability (%) of detecting either two blobs: (●) awareness of the blind spot or a (■) filling-in of the blind spot. Blind spot awareness was reported when the bar lengths extended beyond 0.4° from the edge of the blind spot. Filling-in of the bar was reported when the bar lengths extended 1.25° beyond the edge of the blind spot (75% detection threshold). The *gray area* represents the outer 0.5° of the blind spot, and 0 (zero) represents the temporal edge of the blind spot. Each point is the mean of 50 presentations. Error bars display ±1 SEM.

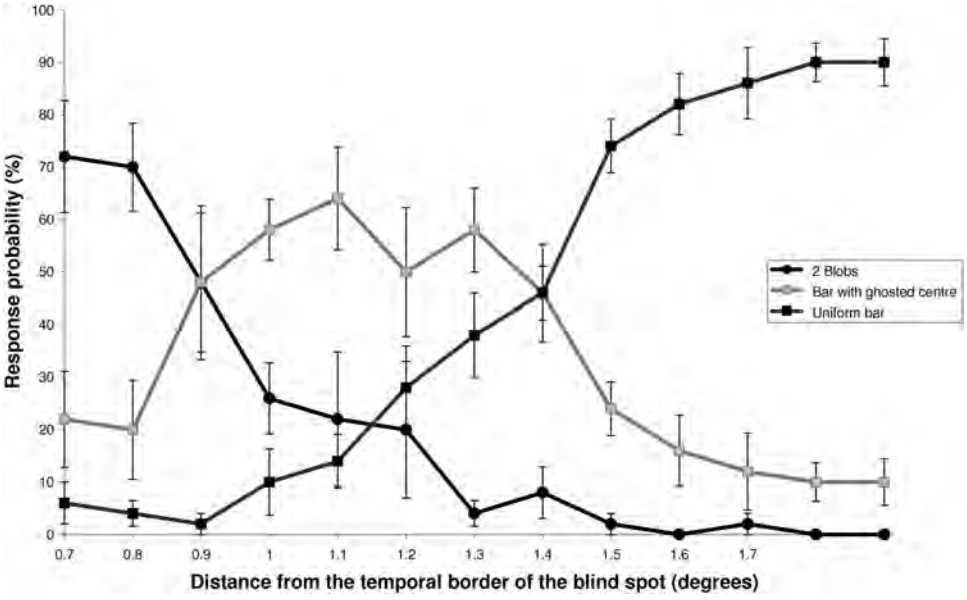

FIGURE 5. Relationship between the length of the bar extending beyond the blind spot boundary and the response probability (%) for blobs (●), a continuous bar with a ghosted center (■), and a uniform bar (■). Ghosted bars are detected over a 0.4° range and reach peak detection for bar lengths of 1.1°. Detection thresholds over 75% for the uniform bar were not recorded until bar lengths exceeded 1.5°. Error bars display ±1 SEM.

thickness at 20-μm intervals from both nasal and temporal edges of the optic nerve head out to 740 μm ($n = 6$) and 1040 μm ($n = 4$). Using Drasdo and Fowler's[20] nonlinear computations of the projections of visual angle to retinal distance, 740 μm and 1040 μm equate to ± 2.57° and 3.61°, respectively.

Photoreceptor Roll-off at the Neuroretinal Rim

To explore the retinal morphology of the roll-off at the neuroretinal rim, we plotted our normalized ONL thickness data (●) alongside the only previously published normalized photoreceptor spatial density data set[18] (●) for a range of temporal retinal eccentricities (Fig. 8). Location sampling differences between the two studies meant only eight data positions were exactly coincident and another was within 10 μm over the 740-μm interval. At the first comparable retinal eccentricity, 100 μm, mean ONL thickness was recorded to be 29.2 ± 5.4 μm. This corresponded to a photoreceptor (i.e., both rods and cones) spatial density of approximately 54,000/mm^2 photoreceptors. At a retinal location of 740 μm from the temporal edge of the optic nerve head, ONL thickness and photoreceptor density values had reached over 90% levels at 61.0 μm and 137,000/mm^2, respectively.

Retinal Limits of Awareness and Filling-in of the Blind Spot

In our present study, we have shown that awareness of the blind spot is likely when a stimulus bar falls on 115 μm retinal

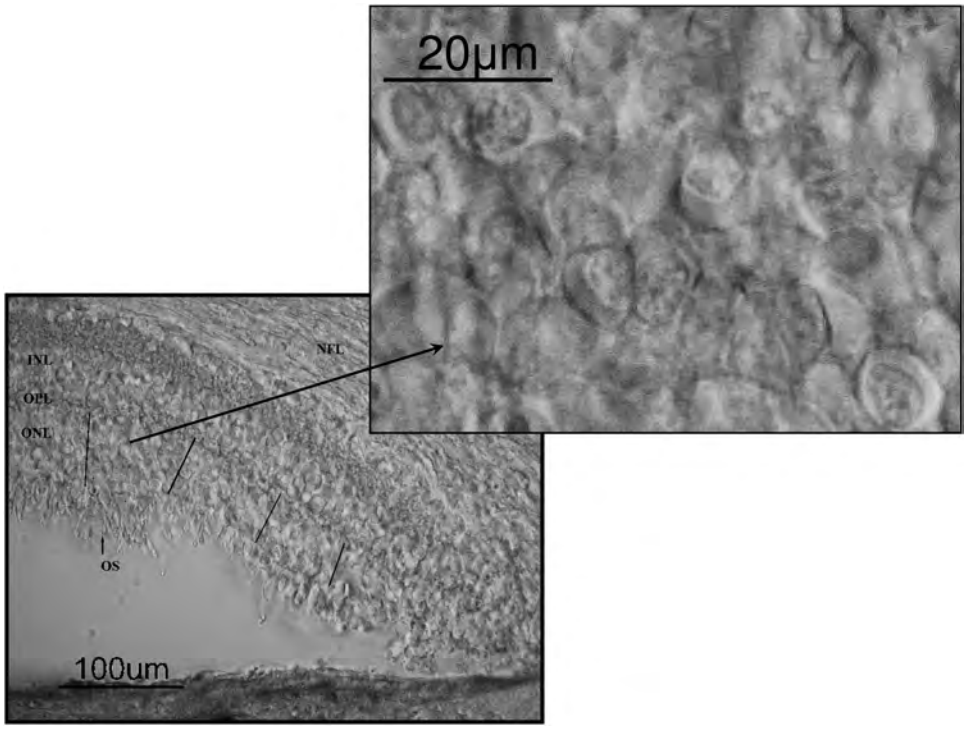

FIGURE 6. Light microscope image using DIC optics showing a section through human retina adjacent to the nasal rim of the optic nerve head. A magnified section of the outer nuclear layer is shown in the upper right panel. OS, outer segment layer; ONL, outer nuclear layer; OPL, outer plexiform layer; INL, inner nuclear layer; NFL, nerve fiber layer.

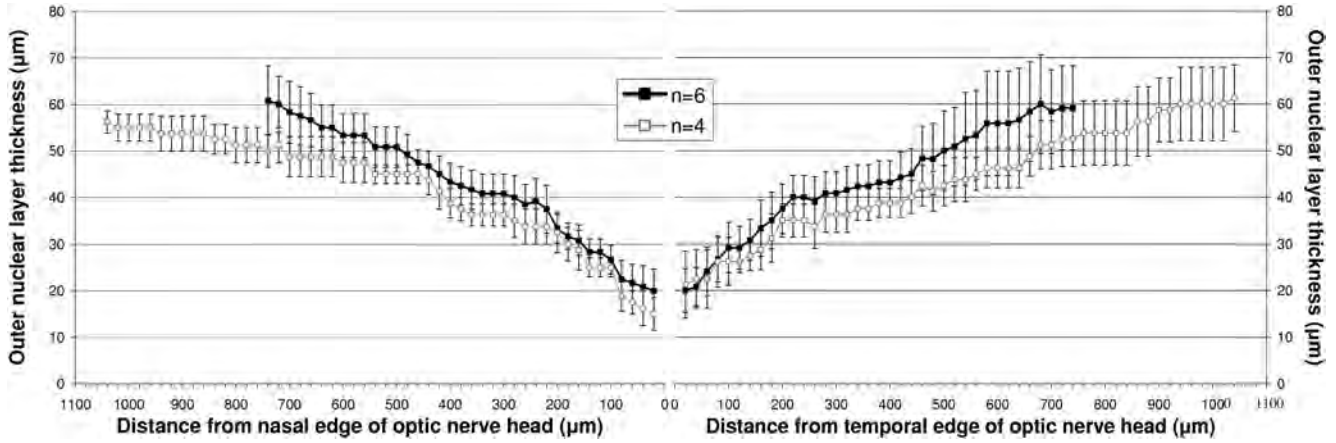

FIGURE 7. The relationship between the thicknesses of healthy human ONL as a function of eccentricity from the rim of the optic nerve. Nasal and temporal borders of the optic nerve are represented by 0. Data were collected at intervals of 20 μm up to 740 μm from six donor eyes (■) and up to 1040 μm for 4 of 6 donor eyes (□). Error bars display ±1 SEM.

tissue adjacent to and on either side of the optic nerve. This corresponded to a visual angle of 24 min arc and is the first quantification of blind spot awareness using a predominantly intrinsic stimulus.

Conventionally, monocular blind spot filling-in has been explored by using visual stimuli placed predominantly outside the blind spot to generate an illusory percept within the region of space where there are no photoreceptors. Such a filling-in phenomenon has generally been considered an "all-or-none" behavior.[6–9] Subjectively, when features such as extrinsic collinear bars invaded the blind spot, subjects became aware of the completion. However, no indication has been given as to whether the completion is partial or complete. In comparison, our present study has explored two discrete aspects of filling-in by varying the response criteria (i.e., ghosted and uniform bar). In this way we were able to explore the impact of top-down influences on our threshold responses.

Our study also sought to determine the spatial limits of retinal stimulation needed to drive filling-in, and we identified a 0.5° range between 1.0° (288 μm) and 1.5° (432 μm), which encompassed both partial and total filling-in. As stated earlier (see Results: Experiment 2), the experimental methodology can strongly influence the spatial extent of filling-in.

In comparison, a recent study[14] using a narrow concentric ring of texture immediately bordering the blind spot (Fig. 1b) found that total filling-in of the blind spot was reported for widths of the annulus between 20 min arc and 40 min arc (i.e., 96–192 μm). However, our study design differed in a number of significant ways from the design of that study.[14] First, we mapped out the position and size of the blind spot using a stationary target presented in time rather than using a moving target (kinetic mapping). The latter method can introduce reaction time artifacts and result in misleading blind spot topographies. Second, the location of our stimulus was predominantly intrinsic rather than exclusively extrinsic to the blind spot, thereby minimizing adaptation and eye movement confounds. Third, we chose to use bar stimulus, which is more local than the global annulus used by Spillman et al. [14] Fourth, our study was able to make apparent the confound of top-down influences by examining partial as well as total filling-in of the blind spot.

Initial blind spot awareness was judged to occur when the two separate blobs were first detected (Fig. 2c). Using the weighted function of ONL thickness (Fig. 8 ◇) and photoreceptor data, we found a blind spot awareness range that corresponded to retinal distances between 24 min arc and 48 min

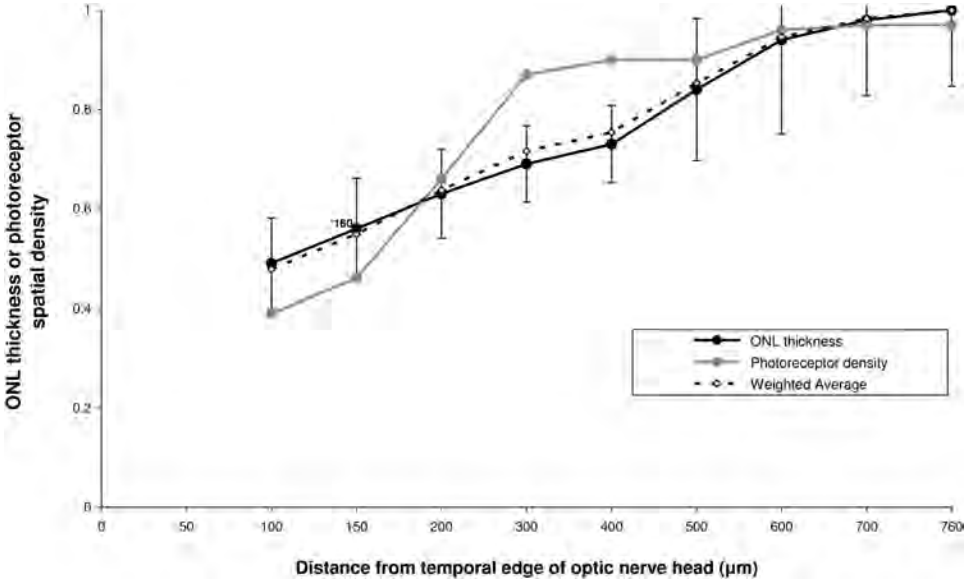

FIGURE 8. Normalized nasal ONL thickness data from this study (●) plotted alongside the spatial density of the nasal retinal photoreceptors (rods and cones; ●) taken from the 1990 study by Curcio et al.[18] for retinal locations between 100 μm and 740 μm from the temporal rim of the optic nerve head. A weighted average of the two functions is shown (◇). SEM is shown only for the ONL thickness data (n = 6). Photoreceptor density data are taken from a single eye.

arc (115–230 μm), reflecting a need to stimulate between 48% and 63% of the maximum spatial density of photoreceptors. Partial bar filling-in (i.e., a bar with a ghosted center; Fig. 2d) began at approximately 66 min arc and continued to 78 min arc (317–374 μm) and corresponded approximately to 72% to 76% of the maximum photoreceptor spatial density. Total filling-in (i.e., a uniform bar; Fig. 2e) was found to occur beyond 90 min arc (432 μm; corresponding to approximately 78% of the maximum photoreceptor spatial density).

Most of the prevailing evidence suggests that there are strong, active mechanisms in the visual cortex underpinning this behavior.[13,17,21–24] However, lower order afferents that drive the cortical responses also merit consideration.

Phenomenology of Visual Scotoma

Over the years a broad range of modal and amodal filling-in categories have been investigated.[7] These may be classed as physiological (e.g., the blind spot, a simulated scotoma within a visual scene, illusionary modal contours [i.e., Kaniza triangle]) or pathologic, secondary to disease or trauma along the visual pathway. In the case of the physiological blind spot, previous studies have demonstrated that visual field loss is not an isolated absolute scotoma but is an ellipsoid absolute scotoma surrounded by a relative scotoma annulus.[25–28] Psychophysically, this relative area can be demarcated using small stimuli subtending 30 min arc. Supporting evidence for this sensitivity gradient comes from the histologic mapping of photoreceptor density at the neuroretinal rim, which can extend beyond 62.5 min arc (300 μm),[18] together with perimetric studies showing a shoulder of at least 44 min arc (211 μm) from the blind spot.[25–28] Our ONL thickness data (Fig. 7) also lend support to this view. However, it should be emphasized that histologic studies are prone to large intersubject variability, with differences in tissue preparation and sampling making comparisons difficult.[18,29,30]

In summary, compared with other categories of completion, the blind spot is clearly a special case. The visual pathways are intact and the photoreceptor gap is hard wired. Moreover, the blind spot scotoma is fixed and located approximately 15° temporal to fixation. It also exhibits a relative sensitivity gradient around the absolute central scotoma. Yet, and almost certainly because of these unique conditions, the predictable visual consequences do not readily enter our consciousness during natural viewing conditions. For larger surrounds, contour completion across the blind spot is immediate, sustained, and apparently effortless, although in common with other categories of filling-in it is unlikely to be an accurate representation of the missing scene.

Concluding Remarks

Filling-in of the blind spot involves neural interpolation across the photoreceptor-free zone. In the past, cortical neural mechanisms underlying this behavior have emphasized the role of neuronal firing rates in the retinotopically organized areas of V1 and V2[31–34] and the need to consider processing far beyond the "classical" receptive field.[32,35,36] To date, explanations for awareness and filling-in of the blind spot have tended to neglect the precortical stages of neuronal processing. The primary purpose of the present study was to link the perceptual experience with the corresponding retinal neuroanatomy. Here we have provided direct evidence that variation in photoreceptor density around the neuroretinal rim should be taken into account in future psychophysical explanations. Moreover, incorporating aspects of retinal structure and function, together with aspects of neural activity in the visual cortex and subsequent cognitive processing (attention, inference, and salience) is likely to assist further understanding of the underlying mechanisms responsible for the spatial and temporal limits to awareness and filling-in of the blind spot.

Acknowledgments

The authors thank the staff of the Moorfields Eye Bank, and Richard Clement, Gillian Connor, Christine Curcio, and Ellen Lee for helpful discussions.

References

1. Polyak SL. *The Retina*. Chicago: University of Chicago; 1941.
2. Hogan MJ, Alvarado JA, Weddell JE. *Histology of the Human Eye*. Philadelphia: WB Saunders; 1971.
3. Fine BS, Yaroff M. *Ocular Histology*. New York: Harper & Row; 1972.
4. Andrews PR, Campbell FW. Images at the blind spot. *Nature.* 1991;353:308.
5. Ferree CE, Rand G. The spatial values of the visual field immediately surrounding the blind spot and the question of the associated filling in of the blind spot. *Am J Physiol.* 1912;29:398–417.
6. Walls GL. The filling-in process. *Am J Optom Arch Am Acad Optom.* 1954;31:329–341.
7. Pessoa L, De Weerd P, eds. *Filling-in: From Perceptual Completion to Cortical Reorganisation*. Oxford: Oxford University Press; 2003.
8. Ramachandran VS. Filling-in the blind spot. *Nature.* 1992;356:115.
9. Kawabata N. Visual information processing at the blind spot. *Percept Motor Skills.* 1982;55:95–104.
10. Tripathy SP, Levy DM. Perceptual distortions and cortical binocular interactions around the blind spot. *Invest Ophthalmol Vis Sci.* 1993;34:794.
11. Tripathy SP, Levi DM, Ogmen H. Two-dot alignment across the physiological blind spot. *Vis Res.* 1996;36:1585–1596.
12. Pessoa L, Thompson E, Noë A. Finding out about filling-in: a guide to perceptual completion for visual science and the philosophy of perception. *Behav Brain Sci.* 1998;21:723–802.
13. Fiorani M Jr, Rossa MGP, Gattass R, Rocha-Miranda CE. Dynamic surrounds of receptive fields in primate striate cortex: a physiological basis for perceptual completion? *Proc Nat Acad Sci U S A.* 1992;89:8547–8551.
14. Spillman L, Otte T, Hamburger K, Magnussen S. Perceptual filling-in from the edge of the blind spot. *Vision Res.* 2006;46:4252–4257.
15. Horton JC, Hocking DR. Intrinsic variability of ocular dominance columns in normal macaque monkeys. *J Neurosci.* 1996;16:7228–7239.
16. Horton J, Dagi LR, McCrane EP, De Monasterio FM. Arrangement of ocular dominance columns in human visual cortex. *Arch of Ophthalmol.* 1990;108:1025–1031.
17. Komatsu H, Kinoshita M, Murakami I. Neural responses in the retinotopic representation of the blind spot in the macaque V1 to stimuli for perceptual filling-in. *J Neurosci.* 2000;20:9310–9319.
18. Curcio CA, Sloan KR, Kalina RE, Hendrickson AE. Human photoreceptor topography. *J Comp Neurol.* 1990;292:497–523.
19. Østerberg GA. Topography of the layer of the rods and cones in the human retina. *Acta Ophthalmol.* 1935;13(suppl 6):1–103.
20. Drasdo N, Fowler CW. Non-linear projection of the retinal image in a wide-angle schematic eye. *Br J Ophthalmol.* 1974;58:709–714.
21. De Weerd P, Gattass R, Desimone R, Ungerleider L. Responses of cells in monkey visual cortex during perceptual filling-in of an artificial scotoma. *Nature.* 1995;377:731–734.
22. Murakami I. Motion after effect after monocular adaptation to filled-in motion at the blind spot. *Vision Res.* 1995;35:1041–1045.
23. Komatsu H. The neural mechanisms of perceptual filling-in. *Nat Rev Neurosci.* 2006;7:220–231.
24. Tootell RBJ, Hadjikhani NK, Vanduffel W et al. Functional analysis of primary visual cortex (V1) in humans. *Proc Nat Acad Sci U S A.* 1998;95:811–817.
25. Jonas JB, Gusek GC, Fernández MC. Correlation of the blind spot size to the area of the optic disc and parapapillary atrophy. *Am J Ophthalmol.* 1991;111:559–565.
26. Jonas JB, Nguyen XN, Gusek GE et al. Parapapillary choroidal atrophy in normal and glaucomatous eyes. *Invest Ophthalmol Vis Sci.* 1989;30:908–918.

27. Meyer JH, Guhlman M, Funk J. Blind spot size depends on the optic disc topography: a study using SLO controlled scotometry and the Heidelberg retina tomography. *Br J Ophthalmol.* 1997;81: 355–359.
28. Rensch F, Jonas JB. Direct microperimetry of alpha and beta zone parapapillary atrophy. *Br J Ophthalmol.* 2008;92:1617–1619.
29. Curcio CA, Millican CL, Allen KA, Kallina RE. Aging of the human photoreceptor mosaic: evidence for the selective vulnerability of rods in central retina. *Invest Ophthalmol Vis Sci.* 1993;34:3278–3296.
30. Curcio CA. Photoreceptor topography in ageing and age-related maculopathy. *Eye.* 2000;15:376–383.
31. Von der Heydt R, Peterhans E, Baumgartner G. Illusory contours and cortical neuron responses. *Science.* 1984;224:1260–1262.
32. Zipster K, Lamme VA, Schiller PH. Contextual modulation in primary visual cortex. *J Neurol.* 1996;16:7376–7389.
33. Meng M, Remus DA, Tong F. Filling-in of visual phantoms in the human brain. *Nat Neurosci.* 2005;8:12481254.
34. Cornelisson FW, Wade AR, Vladusich T et al. No functional magnetic resonance imaging evidence for brightness and colour filling-in in early human visual cortex. *J Neurosci.* 2006;26:3634–3641.
35. Spillman L, De Weerd P. Mechanisms of surface completion: perceptual filling-in of texture. In: Pessoa L, De Weerd P, eds. *Filling-in: From Perceptual Completion to Cortical Reorganisation*. Oxford: Oxford University Press; 2003;81–95.
36. Spillman L. From perceptive fields to Gestalt. In: Martinez-Conde S, Macknick S, Martinez LM, Alonso J-M, Tse PU, eds. *Progress in Brain Research. Volume 155. Visual Perception Part 2: Fundamentals of Awareness, Multi-Sensory Integration and High-Order Perception.* Elsevier; 2006:67–91.